

01 Jan 2007

## Development and Application of a High-Resolution Thin-Film Probe

Shaohua Li

Kuifeng Hu

Daryl G. Beetner

*Missouri University of Science and Technology, daryl@mst.edu*

James L. Drewniak

*Missouri University of Science and Technology, drewniak@mst.edu*

*et. al. For a complete list of authors, see [https://scholarsmine.mst.edu/ele\\_comeng\\_facwork/1540](https://scholarsmine.mst.edu/ele_comeng_facwork/1540)*

Follow this and additional works at: [https://scholarsmine.mst.edu/ele\\_comeng\\_facwork](https://scholarsmine.mst.edu/ele_comeng_facwork)



Part of the [Electrical and Computer Engineering Commons](#), and the [Materials Science and Engineering Commons](#)

---

### Recommended Citation

S. Li et al., "Development and Application of a High-Resolution Thin-Film Probe," *Proceedings of the IEEE International Symposium on Electromagnetic Compatibility (2007, Honolulu, HI)*, Institute of Electrical and Electronics Engineers (IEEE), Jan 2007.

The definitive version is available at <https://doi.org/10.1109/ISEMC.2007.47>

This Article - Conference proceedings is brought to you for free and open access by Scholars' Mine. It has been accepted for inclusion in Electrical and Computer Engineering Faculty Research & Creative Works by an authorized administrator of Scholars' Mine. This work is protected by U. S. Copyright Law. Unauthorized use including reproduction for redistribution requires the permission of the copyright holder. For more information, please contact [scholarsmine@mst.edu](mailto:scholarsmine@mst.edu).

# Development and Application of a High-Resolution Thin-Film Probe

Shaohua Li, Kuifeng Hu, Daryl Beetner, James  
Drewniak, James Reck, Matt O'Keefe  
UMR Electromagnetic Compatibility Laboratory  
University of Missouri - Rolla  
Rolla, MO, USA  
daryl@umr.edu

Kai Wang, Xiaopeng Dong, Kevin Slattery  
Corporate Technology Group  
Intel Corporation  
Hillsboro, OR 97124  
Kevin.p.slattery@intel.com

**Abstract** – This paper documents the development, characterization, and application of a high-resolution thin-film magnetic-field probe. Probe diameter ranged from 5- $\mu\text{m}$  to 100- $\mu\text{m}$ . The 100- $\mu\text{m}$  probe exhibits a 250- $\mu\text{m}$  improvement in spatial resolution compared to a conventional loop probe, measured at a height of 250  $\mu\text{m}$  over differential traces with a 118- $\mu\text{m}$  spacing. Electric field rejection was improved using shielding and using a 180-degree hybrid junction to separate common-mode (electric field) and differential-mode (primarily magnetic field) coupling. A network analyzer with narrow band filtering was used to detect the relatively weak signal from the probe and to allow detection of phase information. An application of the probe is demonstrated where the probe is used to identify the magnitude and phase of magnetic fields produced by currents in very closely-spaced IC package pins.

**Keywords** - Thin-film devices; scanning antennas; probe antennas; electromagnetic compatibility; electromagnetic interference.

## I. INTRODUCTION

Near-field measurements are useful for debugging electromagnetic compatibility problems, for understanding the distribution of high-frequency currents within a printed circuit board or the package of an integrated circuit (IC), and for determining the potential of an IC to cause radiated emissions [1],[2]. There are two major challenges to developing magnetic field probes for near-field scanning of ICs: obtaining the high spatial-resolution necessary to differentiate structures within the IC while maintaining sensitivity and obtaining accurate measurements of the magnetic field independent of the electric field. Both spatial resolution and accurate measurement of the fields can be improved using calibration and compensation procedures [3]. The influence of the electric field can also be reduced using shielding structures [4] or by using symmetric sensors to couple both electric and magnetic fields and then separating the influence of the fields through the measurement technique [5]. In the latter case, differential and common mode signals are separated by measuring the magnitude and phase of three S-parameters and then calculating  $(S_{21}-S_{31})/2$  and  $(S_{21}+S_{31})/2$ . The measurement system requires a three-port network analyzer and a synchronization of signals that is

not always available. The most direct way to improve spatial resolution is to minimize the size of the probe.

This paper presents the development and application of a thin-film probe with a small loop size and improved spatial resolution compared to a conventional loop probe. The following paragraphs explain the design and fabrication of the probe, present its measured electrical characteristics, and illustrate the utility of the probe through measurement of the near-magnetic fields over the pins of an IC in a package with closely spaced pins. The text also outlines measurement techniques to help improve electric-field rejection and to measure the phase of magnetic fields over an operating circuit.

## II. PROBE DESIGN

A layout of one probe along with its dimensions is shown in Fig.1. The probe was constructed using a series of thin-film photolithography processes [6],[7]. A thin layer of silver was deposited on a silicon base and then was etched to form the traces and loop that constitute the main part of the probe. The traces were covered with an insulating material, SU-8, which is commonly used as part of many specialty photolithography processes. An additional layer of silver was patterned on top of the SU-8 to form a shield. The wafer was diced to separate individual probes. A single die including a probe was then washed in a chemical bath to separate the silver and SU-8 from the silicon base, thus forming a probe from the shield, SU-8, and traces, with the SU-8 acting as an insulator between the two metal layers. By removing the probe from the silicon, one obtains a probe that is flexible enough to temporarily deform after unintentional contact with the device under test while still maintaining structural integrity. Silicon would be too brittle under these conditions and has the added drawback that it is difficult to cut the silicon in such a way to allow the probe to be placed very close (closer than the diameter of the probe) to the device under test.

After construction, the thin film probes were bonded to a prefabricated printed circuit board (PCB) that connects the probe to the test equipment. Pictures of the probe connections and of the PCB are shown in Fig. 2 and 3. After cleaning, the probe shield was attached to the ground plane of the PCB using an electrically conductive epoxy.

Following a complete cure of the ground plane-epoxy connection, bonding pads on the probe traces were attached to matching bonding pads on the PCB using gold wire. The gold wire was attached by hand using an electrically conductive epoxy and a microscope. Optical micrographs of the final probe assembly are shown in Fig. 4.

Five different probes were fabricated with trace widths ranging from 100  $\mu\text{m}$  to 5  $\mu\text{m}$ , and line spacings ranging from 60  $\mu\text{m}$  to 5  $\mu\text{m}$ , respectively. Here, we report testing of the probe with a 100  $\mu\text{m}$  trace width and a 60  $\mu\text{m}$  line spacing.

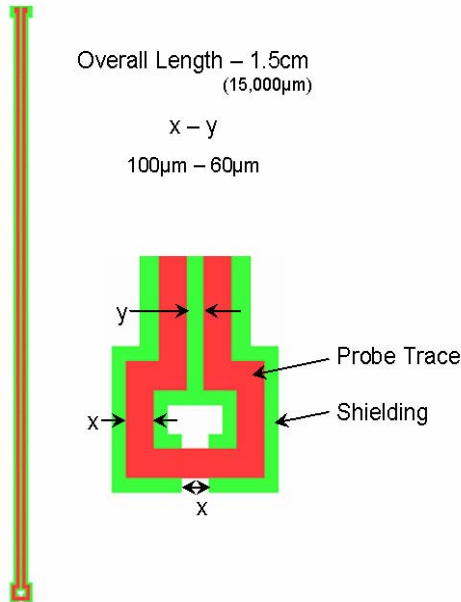


Fig. 1. Layout of the thin-film probe.

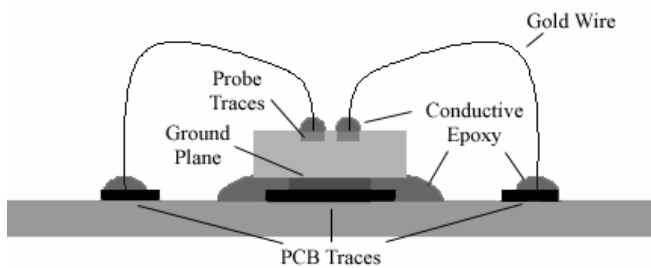


Fig. 2. Cross section of bonded probe.

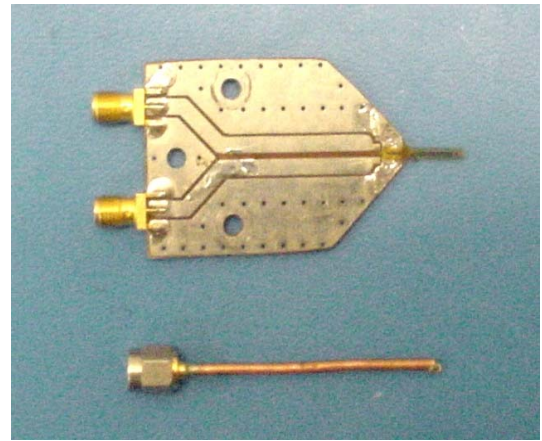


Fig. 3. The thin-film probe and a simple loop probe.

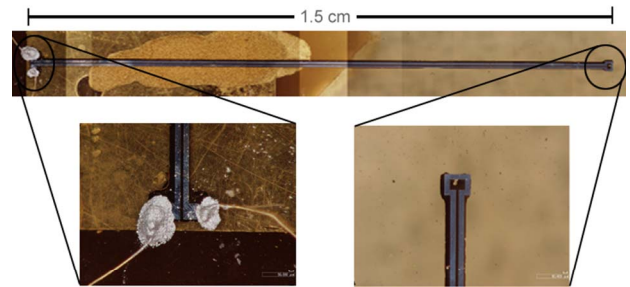


Fig. 4. Optical micrographs of the probe. Top: a compilation of several images showing the full length of the 100- $\mu\text{m}$  probe. Lower left: a magnified view of the wire bonds. Lower right: a close-up of the probe tip.

### III. CHARACTERIZATION OF THE PROBE

#### A. Measurement Setup

The electrical characteristics of the probe were measured using the setup shown in Fig. 5. An AMP 96341 40 dB hybrid was used to help separate electric- from magnetic-field coupling. A differential mode current is created on the two probe traces when a magnetic field couples to the probe through the loop-tip. Electric field coupling primarily produces a common mode current. The hybrid was connected to better measure the differential current produced by the magnetic field. The hybrid was designed to work from 2 MHz – 2 GHz. Low noise amplifiers were inserted between the hybrid and the probe to improve sensitivity.

The frequency response of the probe was measured in three steps. The first step was to measure the response of the hybrid and low noise amplifiers for de-embedding purposes, as shown in block one of Fig. 5. An HP 8720 ES four-port network analyzer was used to measure the single-ended three-port S-parameters from Port C1, Port C2 and Port D as indicated in the figure. These measurements were then transformed into mixed mode S-parameters [8]. A 20 dB attenuator was used at the output of the amplifier to prevent overloading the network analyzer.

In the second step, a two-port short-open-load-through calibration was made at Port T and Port D, as shown in Fig. 5.

The response of the probe was measured in the third step. The 50-ohm trace was connected to the network analyzer through a 10 dB attenuator to reduce mismatch. The input power of the network analyzer was set to 10 dBm and the resolution bandwidth was reduced to 100 Hz to achieve a low noise floor and allow better measurements at low frequencies. The trace was terminated with a 50 Ω load at Port T. The thin film probe was placed 250 μm above the trace. The frequency response of the probe was calculated by combining the results from steps 1-3. Fig. 6 shows the frequency response of the 100 μm thin-film probe. The data shows a linear frequency response up to 600 MHz with a slope of 20 dB/decade and a usable frequency range up to 2 GHz (the limit of the hybrid used in this experiment).

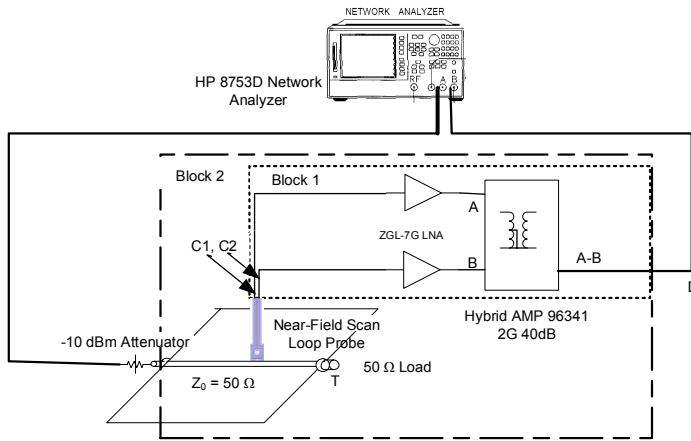


Fig. 5. Measurement setup.

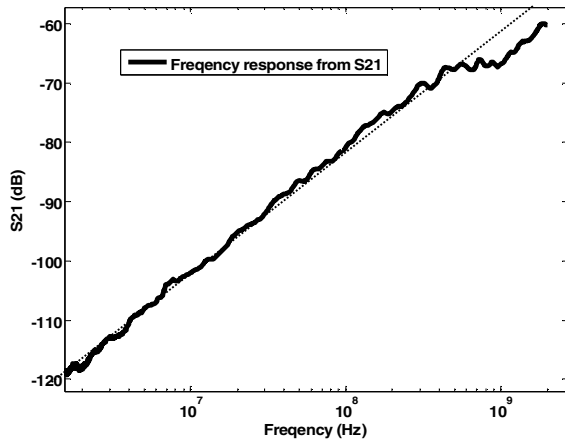


Fig. 6. Measured frequency response.

## B. Spatial Resolution

The spatial resolution of the probe, relative to a typical loop probe, was determined by scanning the probe across a pair of differential traces. The reference probe is shown in Fig. 4. It has a loop area of approximately 1 mm<sup>2</sup>. Ideally, the measurement will show a strong, narrow peak in the magnetic field over each trace that reduces quickly to zero between the traces. The width of the peak over the traces and the null between them is an indication of spatial resolution.

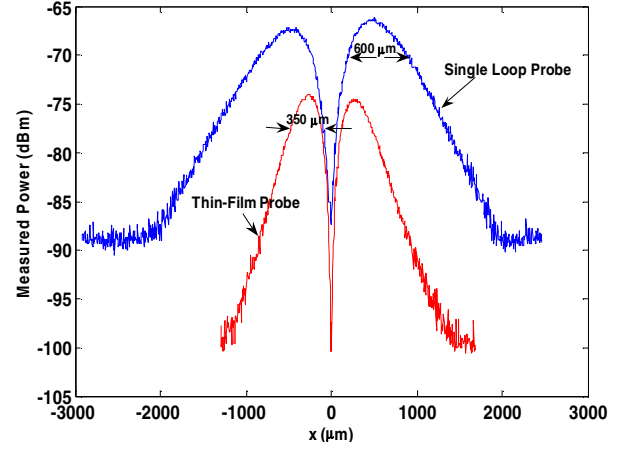


Fig. 7. Comparison of the spatial resolution of the thin-film probe and of a simple loop probe.

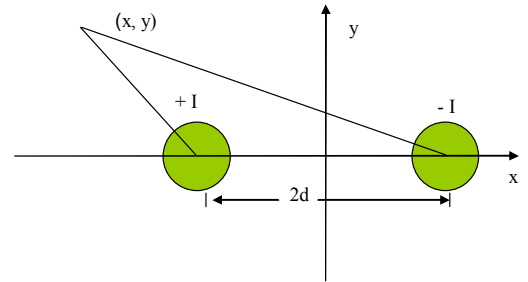


Fig. 8. Model for the magnetic field produced by a differential pair.

The thin-film probe and the conventional loop probe were scanned across the differential trace at a height of 250 μm. The measured signal power is shown in Fig. 7. The thin film probe has a 3 dB decrease over 350 μm, which is 250 μm less than the conventional loop probe.

The spatial resolution found in Fig. 7 is a function of both the probe size as well as the height above the traces. Consider the differential traces shown in Fig. 8. The position of the loop is indicated at coordinates (x, y). When the plane of the loop is perpendicular to the ground plane and parallel to the longitudinal axis of the trace (as indicated in Fig. 9), only the x component of the magnetic field contributes to the magnetic flux through the loop. The magnetic flux is given by:

$$B_x = \frac{\mu_0 I}{2\pi d} \left( \frac{y/d}{((x/d-1)^2 + (y/d)^2)} - \frac{y/d}{((x/d+1)^2 + (y/d)^2)} \right)$$

The magnitude of the field is determined both by a ratio of the height of the probe to trace separation and the ratio of the horizontal position (x-direction) to trace separation. The effect is illustrated in Fig. 10.

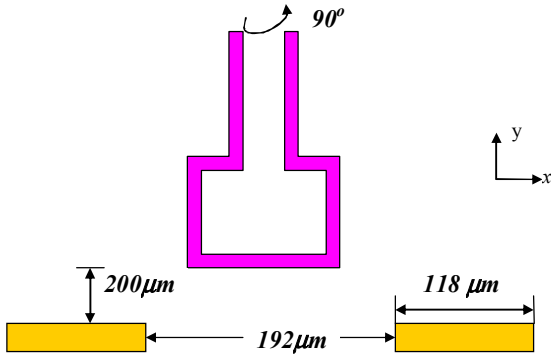


Fig. 9. Measurement of differential traces.

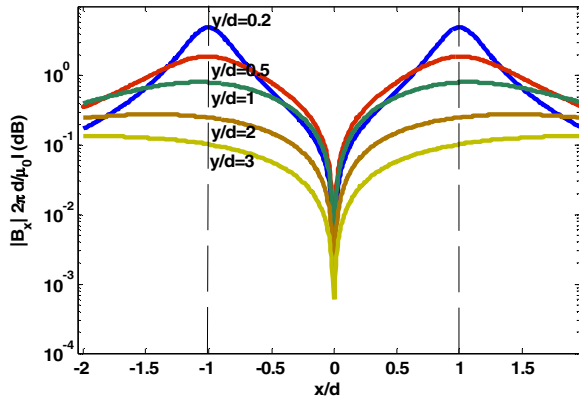


Fig.10. Normalized x component of magnetic field distribution over a pair of differential traces.

### C. Separation of Electric and Magnetic Fields

The ability of the probe and associated measurement setup to separate the magnetic from the electric field was examined by scanning a 7 cm long microstrip trace that was shorted at one end to create a 900 MHz standing wave. Fig. 11 shows the magnitude and phase of the magnetic field over the trace as given by simulation and as measured by the probe. For a pure standing wave, the voltage should reach a maximum at position  $x = 40$  mm and should reach a minimum at  $x = 10$  mm and  $x = 70$  mm. The current is a maximum at  $x = 70$  mm and  $x = 10$  mm and should be zero at  $x = 40$  mm. While the measurement at  $x = 40$  mm (when E is maximum and H is minimum) is not zero, it is about 25 dB lower than a  $x = 10$  mm, illustrating that the probe predominately measures the magnetic field and not the electric field. The phase measurement further confirms this contention, since its value shifts by 180 degrees at the location of a current maximum.

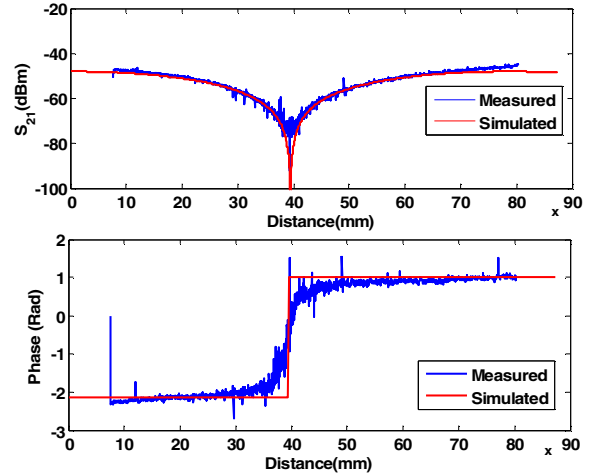


Fig. 11. Measured and simulated power and phase from the thin-film probe over a shorted microstrip trace at 900 MHz. The simulation shows the performance of an ideal magnetic field probe.

## IV. APPLICATION

The thin-film probe was used to measure the magnetic field distribution over the pins of an automotive microcontroller. The microcontroller was in a QFP 100-pin package with closely-spaced pins. Measurements were made at the second harmonic of the 48 MHz clock, i.e. at 96 MHz. The relative phase of magnetic fields over the pins was also measured. Traditionally, phase is measured using an oscilloscope, where signals are measured in the time domain relative to a known signal (such as the microcontroller clock) and then converted to the frequency domain [1]. A side effect of making the probe small is a decrease in sensitivity. The traditional broad-band phase extraction method is not effective for the thin film probe for this reason. To overcome this problem, a measurement setup utilizing a synchronized clock and a network analyzer was developed.

The measurement setup is shown in Fig.12. The microcontroller's clock originates from a Stanford CG635 clock generator. The network analyzer is set to the tuned receiver mode, where the internal reference clock is replaced by the external synchronized signal generator. The signal generator and the center frequency of the network analyzer are set to the same harmonic frequency, 96MHz.  $S_{11}$  was measured for both magnitude and phase. In this case, phase is given relative to the microcontroller clock. The magnitude and phase of the magnetic fields over the 100 pins is shown in Fig. 13. The result shows that the current on the  $V_{dd}$  and  $V_{ss}$  pins are 180 degrees out of phase as expected, with the highest current on  $V_{dd}$  pins 12, 41, 67, and 92. The return current is on  $V_{ss}$  pins 9, 13, 21, 42, 51, 66, 84, and 93. The currents on adjacent  $V_{dd}$  and the  $V_{ss}$  pins do not have the same amplitude, possibly causing an unbalanced current across the package. Such unbalanced currents have been associated with higher TEM cell emissions [9].

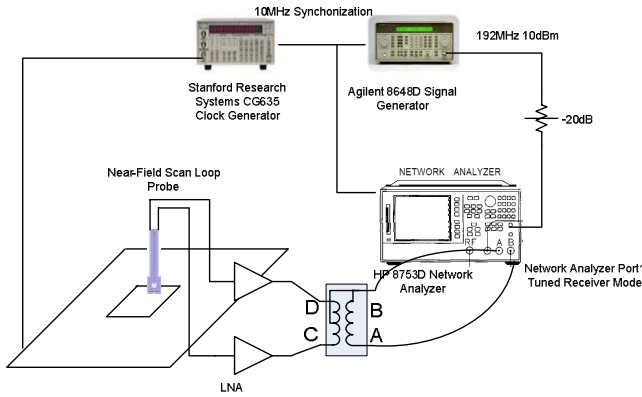


Fig. 12. Setup for measuring magnitude and phase of package-pin currents.

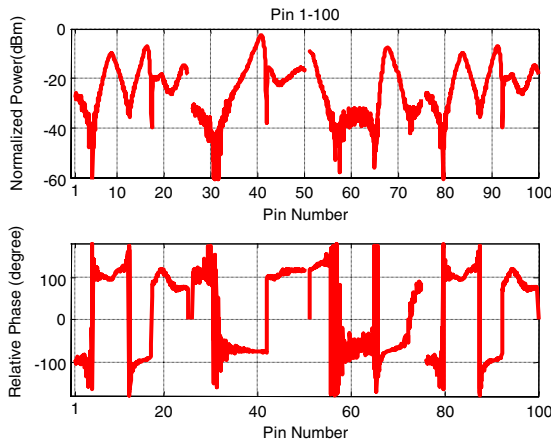


Fig. 13. Magnitude and phase distribution of magnetic fields over package pins, measured at the second harmonic of the clock.

## V. SUMMARY

A thin-film probe with high spatial resolution was developed, characterized and compared to a conventional loop probe. The thin-film probe has a much higher resolution than the conventional probe and measurements show a good separation between electric and magnetic field coupling. Measurement of the magnetic field was improved using a 40 dB hybrid. The probe demonstrated good response up to a 2 GHz, the limit of the working range of the hybrid. Greater range is expected in the future with modifications to the probe and bonding structure as well as the measurement technique. The probe can measure phase as well as the magnitude of magnetic fields using a synchronized, high-resolution clock and a network analyzer. The potential utility of the probe was illustrated through measurements of the magnetic fields over the closely-spaced pins of a microcontroller.

## REFERENCES

- [1] H. Weng, D. G. Beetner, R. E. DuBroff, and J. Shi, "Estimation of High-Frequency Currents from Near-Field Scan Measurements," *IEEE Transactions on EMC*, to appear.
- [2] IEC 61967-3, "Integrated circuits - Measurement of electromagnetic emissions, 150 kHz to 1 GHz - Part 3: Surface Scan Method", 2004.
- [3] J. Shi, M. A. Cracraft, K. P. Slattery, M. Yamaguchi, and R. E. DuBroff, "Calibration and Compensation of Near-Field Scan Measurements," *IEEE Trans. Electromagn. Compat.*, vol. 47, no. 3, August 2005.
- [4] N. Ando, N. Masuda, N. Tarnaki, T. Kuriyama, S. Saito, K. Kato, K. Ohashi, M. Saito, and M. Yamaguchi, "Miniaturized thin-film magnetic field probe with high spatial resolution for LSI chip measurement," *IEEE Int. Symp. EMC*, vol. 2, August 2004.
- [5] S. Kazama and K. I. Arai, "Adjacent Electric Field and Magnetic Field Distribution Measurement System," *IEEE Int. Symp. EMC*, vol. 1, 19-23 Aug. 2002.
- [6] J. Reck, K. Hu, S. Li, M. O'Keefe, J. Drewniak, D. Beetner, et.al., "Fabrication of Two-Layer Thin Film Magnetic Field Micro-Probes on Freestanding SU-8 Photoepoxy," unpublished.
- [7] L.J. Guerin, "The SU-8 Homepage," <http://geocities.com/guerinlj/>.
- [8] D. E. Bockelman, W. R. Eisenstadt, "Combinded Differential and Common-Mode Scattering Parameters: Theory and Simulation," *IEEE Trans. Microwave Theory Tech.*, vol. 43, pp. 1530-1539, July 1995.
- [9] K. Hu, H. Weng, D. Beetner, D. Pommerenke, J. Drewniak, K. Lavery, and J. Whiles, "Application of chip-level EMC in automotive product design," *IEEE Int. Symp. EMC*, pp 842-848, Aug. 2006.